Acta Neuropathol (2004) 107 : 461–474
DOI 10.1007/s00401-004-0837-z

REGULAR PAPER

Shoichi Sasaki · Hitoshi Warita · Tetsuro Murakami
Koji Abe · Makoto Iwata

Ultrastructural study of mitochondria in the spinal cord of transgenic mice with a G93A mutant SOD1 gene

Received: 20 October 2003 / Revised: 26 January 2004 / Accepted: 26 January 2004 / Published online: 17 March 2004

Abstract The purpose of this study was to examine mitochondrial changes in the spinal cord of transgenic mice of a relatively low transgenic copy number (gene copy 10) expressing a G93A mutant human Cu/Zn superoxide dismutase (SOD1) that were generated in our own laboratories by electron and immunoelectron microscopy from presymptomatic to symptomatic stages. Age-matched nontransgenic mice served as controls at each stage. Ultrastructurally, at the early presymptomatic stage, many mitochondria in large myelinated axons exhibited swelling with an increased number of cristae, and bore small vacuoles in the matrix, cristae or both, in the anterior root exit zone, anterior root, and in the neuropils of the ventral portion of the anterior horn. At the late presymptomatic stage, vacuoles of various sizes (including large ones) were observed in the same regions as in the previous stage. The intermembrane space of mitochondria was also vacuolated. In mitochondria with advanced vacuolation, the vacuolar space was filled with a granular or amorphous substance. At the symptomatic stage, mitochondrial vacuolation seen in the late presymptomatic stage persisted, although to a lesser extent. These vacuolated mitochondria were predominantly seen in the axons, but not in the somata of normal-looking neurons or dendrites at any stage, which differs from that described in other reports. Nontransgenic littermates occasionally exhibited vacuolar changes in the axons of anterior horns. However, they were smaller both in size and number than those in transgenic mice. By immunoelectron microscopy using an immunogold labeling method, at the presymptomatic and symptomatic stages both SOD1 and ubiquitin determinants were localized in vacuolated mitochondria, particularly in the granular or amorphous substance of large vacuoles, but were not detected in most normal-appearing mitochondria. The SOD1-immunoreactive mitochondria were exclusively observed in the axons, and not in proximal dendrites or somata. These findings suggest that the toxicity of mutant SOD1 directly affects mitochondria in the axons and increases with the disease progression. Thus, the mutant SOD1 toxicity might disrupt axonal transport of substrates needed for neuronal viability, leading to motor neuron degeneration. The localization of both ubiquitin and SOD1 in vacuolated mitochondria indicates that protein degradation by ubiquitin-proteasomal system may be also disrupted by several pathomechanisms, such as decreased processing of ubiquitinated proteins due to impairment of mitochondrial function or of proteasomal function, both of which are caused by mutant SOD1. Moreover, giant mitochondrial vacuoles occupying almost the entire axonal caliber could be another contributing factor in motor neuron degeneration, in that they could physically block axonal transport.

Keywords Amyotrophic lateral sclerosis · SOD1 mutation · G93A transgenic mice · Mitochondria · Vacuolation

S. Sasaki (✉) · M. Iwata
Department of Neurology, Neurological Institute,
Tokyo Women's Medical University,
8-1 Kawada-cho, Shinjuku-ku, 162-8666 Tokyo, Japan
Tel.: +81-3-33538111 ext 39232, Fax: +81-3-52697324,
e-mail: ssasaki@nij.twmu.ac.jp

H. Warita
Department of Neurology, Yonezawa National Hospital,
Yonezawa, Japan

T. Murakami · K. Abe
Department of Neurology, Okayama University, Okayama, Japan

Introduction

There is accumulating evidence that mitochondria are a major target of mutant Cu/Zn superoxide dismutase (SOD1) toxicity. In mice possessing high copy numbers of the G93A transgene and G37R mutant SOD1 (animal models of human familial ALS), mitochondrial swelling and vacuolation begin at early stages [13, 40] and peak at the onset of muscle weakness [23]. In cultured neuroblastoma cells or motor neurons, expression of mutant SOD1 causes mitochondrial damage and dysfunction [8, 21]. Further-

more, mitochondrial electron transport chain activities are decreased in the anterior horn prior to the disease onset and during the course of disease progression [30]. Thus, mitochondrial abnormalities may play an early role in pathways leading to cell death, or may occur as a consequence of other subtle impairments, and may contribute to mechanisms of chronic neurodegeneration [11]. However, little information is available about morphological changes in mitochondria in SOD1 mutant mice [13, 23, 40]. Previous reports on G93A SOD1 mutant mice show that vacuolated mitochondria are predominantly located in somata or dendrites of motor neurons [13, 20]. In the present study using G93A SOD1 transgenic (Tg) mice with fewer copies (gene copy 10) that were generated in our own laboratories, we report a new finding: mitochondrial vacuolation occurs predominantly in the proximal axons, but not in the somata and dendrites of anterior horn neurons.

Materials and methods

Experimental animals and clinical assessment

Tg mice expressing the G93A mutant human SOD1 [17] were obtained from the Jackson Laboratory (B6SJL-TgN [SOD1-G93A] 1 Gur^{dl}, Bar Harbor, Me., USA) and were backcrossed to a C57BL/6 background strain by mating hemizygote males with inbred C57BL/6 females (C57BL/6CrSlc, Nihon SLC, Shizuoka, Japan), to produce Tg and non-Tg littermates. Backcrossing to the black 6 background entirely eliminated the SJL (dysferlin gene-associated FSH dystrophy) background from the mice used for these studies. The Tg progeny were identified by polymerase chain reaction (PCR) amplification of tail DNA with specific primers for exon 4 [31]. The G93A SOD1 mutant mice expressed relatively low levels of mutant protein (gene copy, 10).

At around 32 weeks of age, the G93A Tg mice developed progressive muscle weakness and spasticity in one or more limbs, beginning in a posterior limb. After 1–2 weeks, they could not feed themselves, due to severe paralysis involving hyperextension of their hind limbs. A total of 14 Tg mice and 12 age-matched non-Tg mice were investigated. The mice were treated in accordance with the declaration of Helsinki and the guiding principles in the care and use of animals.

Histopathological analysis

The Tg and non-Tg mice were examined simultaneously. The Tg mice were divided into three groups: early presymptomatic Tg (age, 24 weeks; n=2), late presymptomatic Tg (age, 28 weeks; n=2), and early symptomatic Tg (age, 32 weeks; n=2). Age-matched non-Tg mice served as controls for each of these groups (n=6). All mice were deeply anesthetized with ether and perfused intracardially with heparinized saline (pH 7.4), followed by perfusion with ice-cold 4% paraformaldehyde (Katayama Chemical, Osaka, Japan) in 0.1 M phosphate buffer (pH 7.4). The spinal cords were removed rapidly and post-fixed by immersion in the same fixative (5 days, 4°C). Cross-sections of the spinal cord were embedded in paraffin, sectioned (4 μm), and stained with hematoxylin and eosin (HE), and Klüver-Barrera stain.

Electron microscopy

Six Tg and six non-Tg wild-type mice were killed at ages ranging from 24 to 32 weeks. All mice were deeply anesthetized with ether and perfused intracardially with heparinized saline (pH 7.4) followed by perfusion with ice-cold 4% paraformaldehyde (Katayama Chemical, Osaka, Japan) and 0.2% glutaraldehyde in 0.1 M phosphate buffer (pH 7.4). The spinal cords were rapidly removed and post-fixed by immersion in the same fixative (5 days, 4°C). Tissues were incubated in 2% osmium tetroxide in 0.1 M cacodylate for 2 h, washed, dehydrated, and embedded in epoxy resin (Epon). Serial semithin sections (1 μm) of whole transversed spinal cords stained with toluidine blue were examined by light microscopy. Appropriate portions of cervical and lumbar spinal cords were cut into ultrathin sections and were stained with lead citrate and uranyl acetate for electron microscopy.

Immunoelectron microscopy

Post-embedding immunogold electron microscopy was performed on spinal cord specimens. Presymptomatic (30 weeks) and symptomatic (35 weeks) mice were deeply anesthetized with ether and perfused intracardially with heparinized saline (pH 7.4) followed by 100 mM phosphate buffer (pH 7.4) containing ice-cold 4% paraformaldehyde and 0.1% glutaraldehyde. Lumbar and cervical spinal cords from fixed mice were removed, dehydrated in 100% ethanol, and embedded in hard grade LR White resin (Electron Microscopy Sciences, Fort Washington, PA) by polymerization overnight at 60°C. Ultrathin sections were cut from the embedded tissue using a microtome, and were collected onto grids (150 mesh). Ultrathin sections were etched in 0.1 N HCl for 5 min, rinsed three times for 5 min each in TBS (20 mM TRIS, 140 mM NaCl, and 2.7 mM KCl, pH 8.0), treated with blocking buffer (0.1% gelatin, 1% normal goat serum, and 0.3% Triton-X-100 in TBS) for 30 min, incubated with the primary antibodies for 2 h at room temperature, rinsed three times for 5 min each in TBS, immersed in gold-conjugated secondary antibody (10-nm gold anti-mouse anti-rabbit) for 1 h, rinsed three times in TBS, rinsed in water, stained with Reynold's lead citrate followed by aqueous 2% uranyl acetate, and dried on filter paper. The following antibodies and sera were used: a rabbit polyclonal anti-human SOD1 antibody [3] at a dilution of 1:500, 1:1,000 or 1:5,000; polyclonal anti-ubiquitin antibody (DAKO) at a dilution of 1:100, 1:500 or 1:1,000; normal rabbit serum (Vector Laboratories).

Results

At the early presymptomatic stage (24 weeks), HE and Klüver-Barrera staining revealed no pathological changes such as vacuolar changes or neuronal loss in the anterior horn neurons. However, on Epon-embedded plastic sections stained with toluidine blue, slight vacuolar changes were observed in the neuropil of the ventral portion of the anterior horn, in the axons of the anterior horn, around the central canal, and in the axons of the anterior root exit zone of the anterior column. Almost all of these vacuoles were small. The lateral and posterior column and the posterior roots showed no abnormality on plastic sections stained with toluidine blue, from either of the two mice.

At the late presymptomatic stage (28 weeks), slight neuronal loss of anterior horn cells was recognized at the cervical (28.0±3.4) and lumbar levels (27.6±5.2), showing significantly lower values than those of the controls (36.1± 2.9, 35.4±2.8, respectively) (P<0.01). On plastic sections, prominent vacuolar changes were observed in the same regions as those remarked in the previous stage (Fig. 1). Proximal swollen axons with prominent vacuolar changes characterized by a sausage or string-of-beads shape were frequently observed in a longitudinal section. Moderate myelin ovoid formation was observed in the anterior, lat-

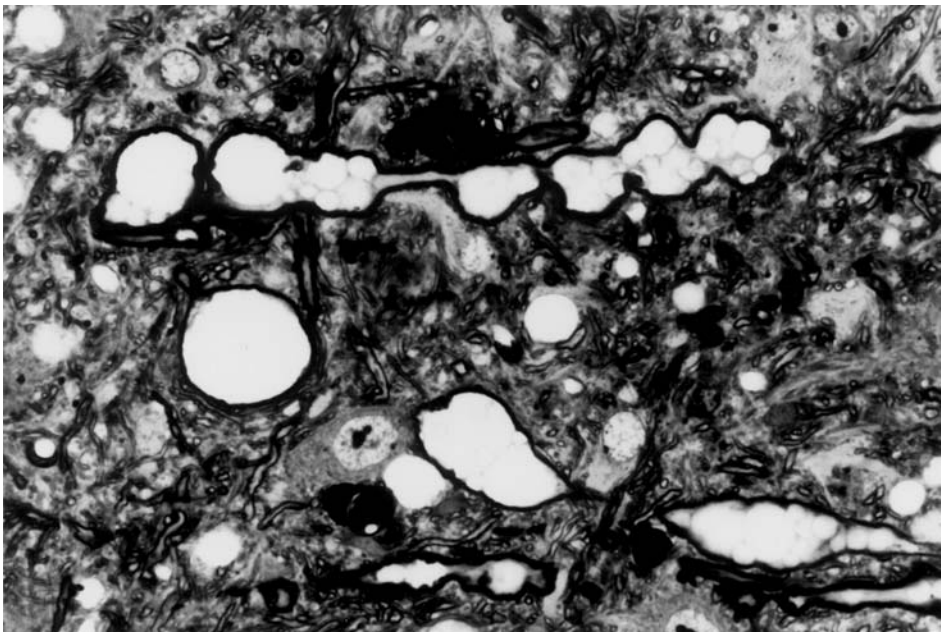

Fig. 1 Vacuolar changes are observed in the axons of the anterior horn and in the neuropil of the ventral portion of the anterior horn (Tg mouse, lumbar cord, 28 weeks) (*Tg* transgenic). ×350

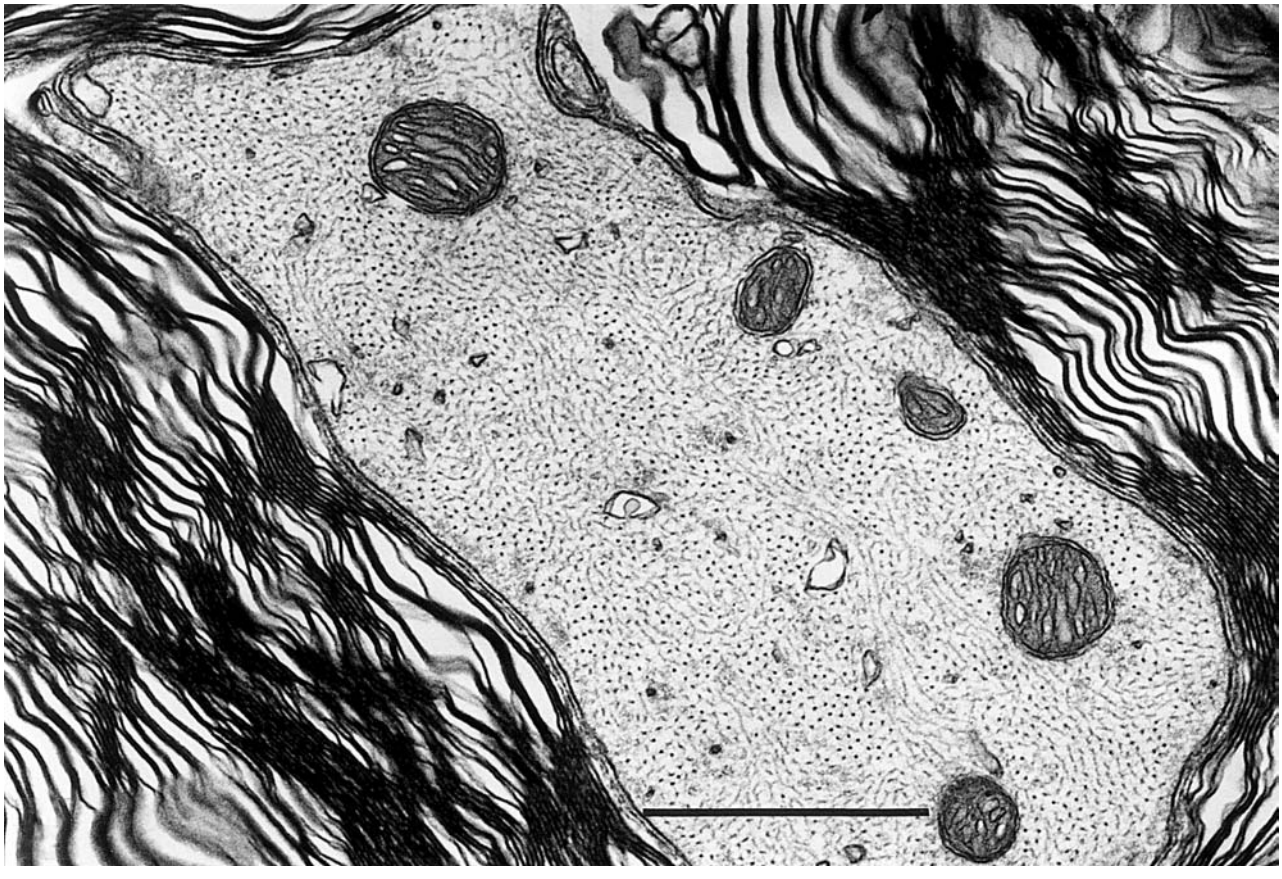

Fig. 2 Normal-appearing mitochondria are visible in the axon of the anterior root in a non-Tg littermate (lumbar cord, 24 weeks). *Bar* 1 μm

eral, and posterior white matter. The anterior roots had degenerated, with vacuolar changes and myelin ovoids, whereas the posterior roots showed no abnormality.

At the symptomatic stage (32 weeks), the anterior horns showed a moderate neuronal loss of anterior horn cells at the cervical (21.8±11.7) and lumbar levels (25.4±4.6); these values were significantly lower than those obtained with the controls (37.4±2.2, 32.9±5.2, respectively) ($P<0.01$). Most remaining anterior horn neurons showed degeneration; e.g., central chromatolysis. On plastic sections, vacuolar changes were less prominent, with the exception of

Fig. 3 Tg mouse (lumbar cord, 28 weeks). **A** Largely swollen mitochondria with an increased number of tubular or vesicular cristae in the axon of the anterior column. **B** Swollen mitochondria with an increased number of tubular cristae in the soma of an anterior horn cell. *Bar* 1 μm

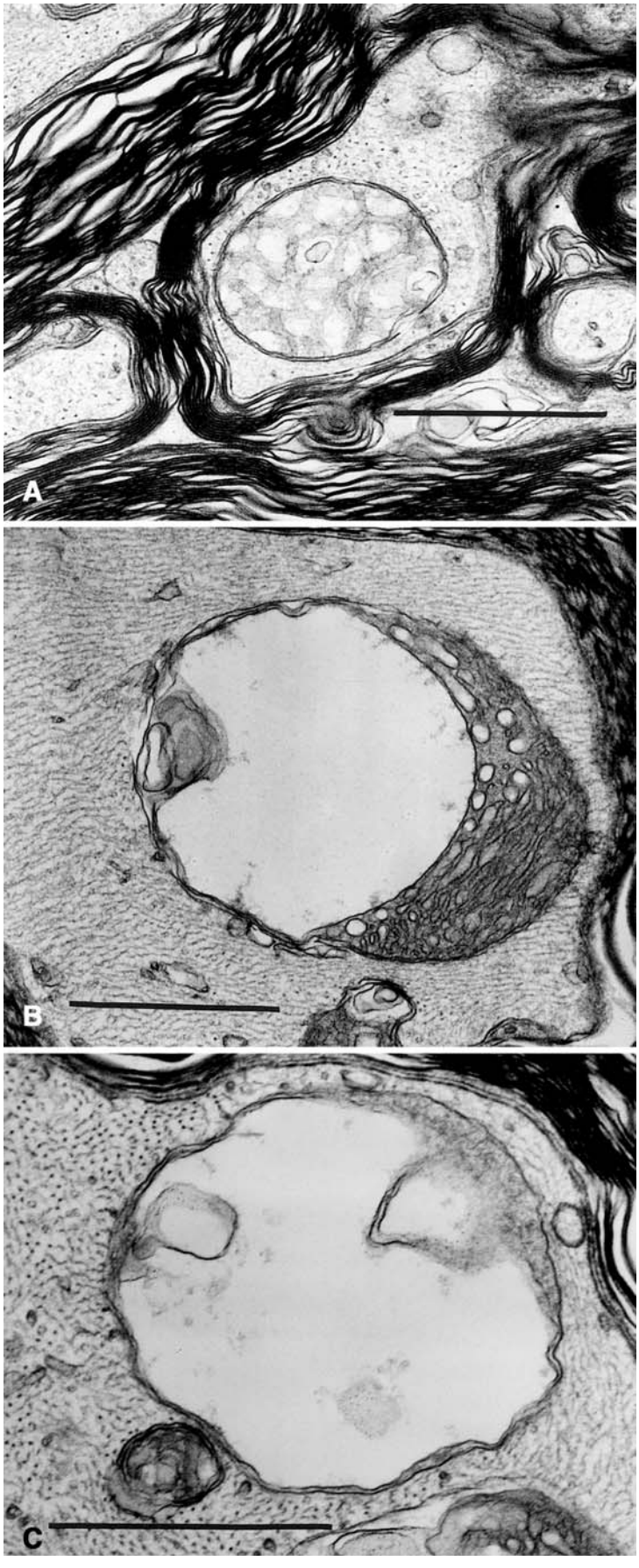

Fig. 4 Tg mouse (lumbar cord, 24 weeks). Vacuolar changes in the inner compartment of mitochondria at the early presymptomatic stage. **A** Dilatation of both the matrix and cristae. **B** Partial vacuolation in the inner compartment. **C** Almost completely disorganized vacuolation in the inner compartment of the matrix and cristae. *Bar* 1 μm

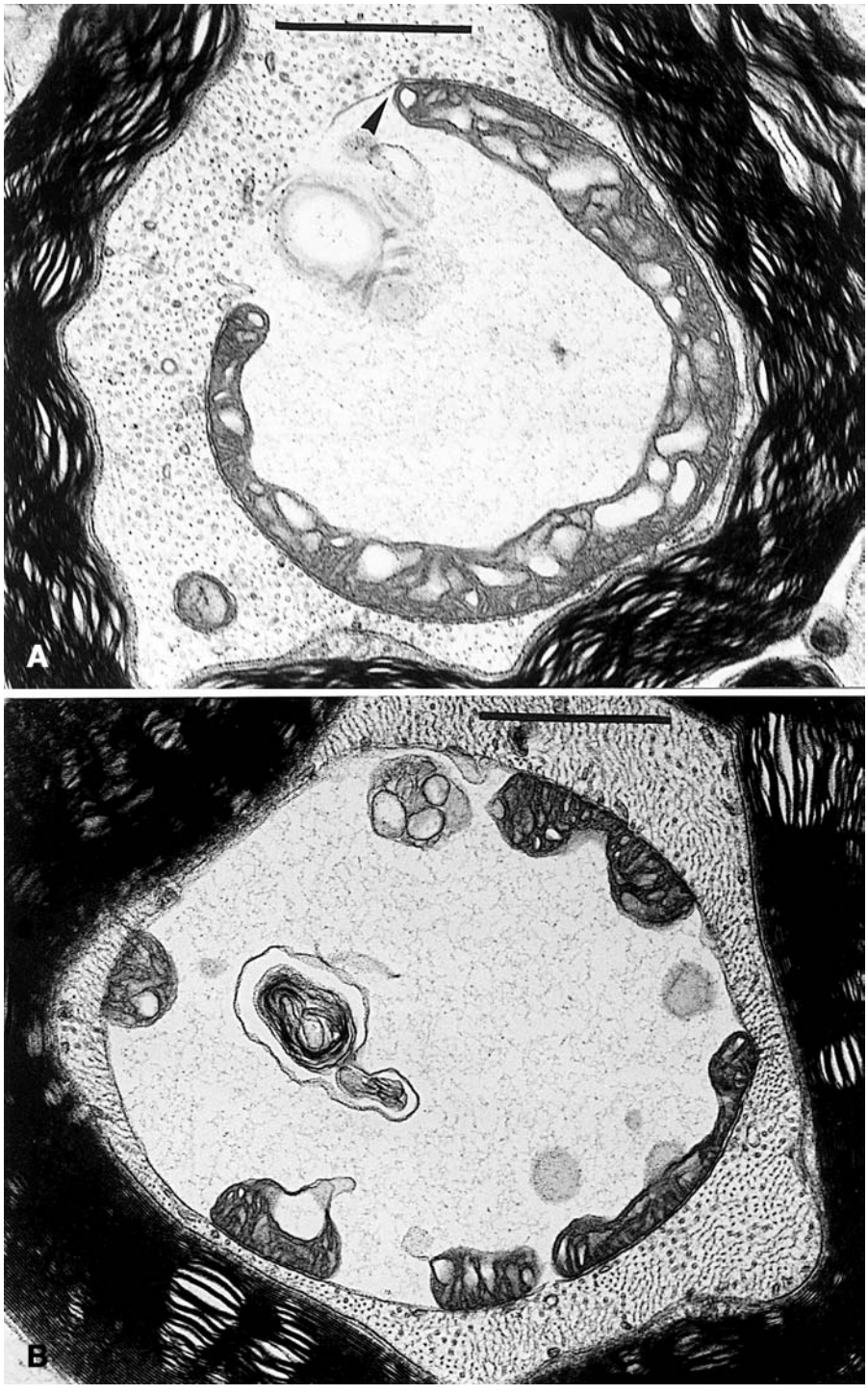

Fig. 5 Tg mouse (lumbar cord, 28 weeks). Vacuolar changes in the intermembrane space at the late presymptomatic stage. The vacuolar space contains a granular or amorphous substance. **A** Dilatation of the intermembrane space (*arrowhead*) with microvacuolation of the inner compartment. **B** Non-vacuolated and vacuolated mitochondria are closely attached to the inner part of the vacuole. *Bar* 1 μm

some that persisted in the anterior root exit zone of the anterior column. Myelin ovoid formation was prominent over white matter of the anterior, lateral (especially at the outer zones of the spinal cord), and posterior columns. In anterior roots, there was marked degenerative change, with marked fiber loss and myelin ovoids, which were definitely worse than in the late presymptomatic stage. To a lesser extent, myelin ovoids were also found in the posterior roots.

Electron microscopic findings

Non-Tg littermates

Mitochondria in perikarya, dendrites and axons were fundamentally similar in structure, although they varied in size and shape. In perikarya and dendrites, they were generally small, rounded, sausage-shaped or slender rodlets. In axons, slender mitochondria predominated, but, in the transverse sections, small globular mitochondria, about

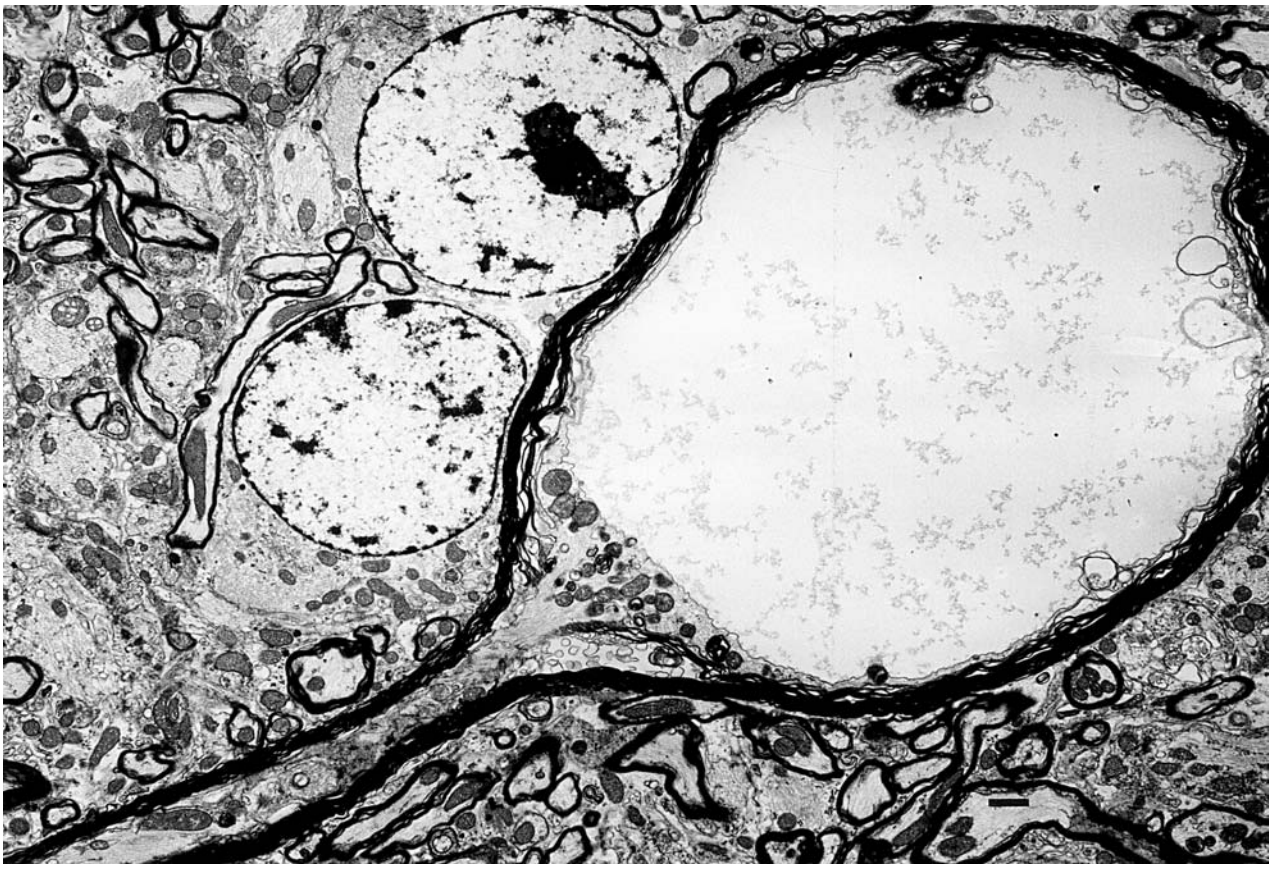

Fig. 6 Tg mouse (lumbar cord, 28 weeks). A giant vacuole occupies the almost entire axonal caliber. The vacuolated space contains a granular or amorphous substance. Mitochondria accumulate in the vicinity of the large vacuole. *Bar* 1 μm

0.1–0.5 μm in diameter, were the most common type (Fig. 2). The mitochondria were surrounded by an outer smooth unit membrane and an inner folded membrane that formed the cristae, which was filled with dense matrix. Spherical or ovoid electron-dense granules were occasionally seen in the matrix. The intermembrane space between the two membranes, the outer mitochondrial compartment, generally had a lucent content. Vacuolar changes were occasionally observed in the axons of anterior horns. These vacuoles were almost always small, and were clearly less common than in Tg mice.

Tg mice

At the early presymptomatic stage, in the anterior root exit zone and anterior root, and in the neuropil of the ventral portion of the anterior horn, the inner compartment of mitochondria exhibited swelling with an increased number of cristae, about 1.7 μm in diameter, frequently in large myelinated axons (Fig. 3A) or, to a lesser extent, in the somata (Fig. 3B) or dendrites. Vacuolar changes (Fig. 4) in the matrix, cristae or both were also observed; these vacuoles consisted of empty spaces of various sizes. Most of these vacuoles were relatively small. In contrast, almost all of the mitochondria in the small myelinated axons in these regions had a normal appearance.

At the late presymptomatic stage, mitochondria were frequently swollen with an increased number of cristae (Fig. 3), and vacuoles were seen in the large myelinated axons in the same regions as in the early presymptomatic stage. Various stages of vacuolar changes, from small focal vacuolar formation in the matrix or cristae to large vacuoles, were observed in these axons. The vacuoles tended to be larger than those of the early presymptomatic stage. The intermembrane space between the inner and outer membranes was also vacuolated (Fig. 5A), with large vacuoles frequently observed. In advanced stages, occasionally non-vacuolated or vacuolated mitochondria were closely attached to the inner part of large single-membrane vacuoles (Fig. 5B). In mitochondria with advanced vacuolation, the vacuolar space was filled with a granular or amorphous substance (Fig. 5). Occasionally, giant vacuoles occupied almost the entire axonal caliber blocking the axonal transport such as mitochondria (Fig. 6). No vacuoles contained intermediate filaments in their interior. In some mitochondria, both the inner compartment and intermembrane space were vacuolated. Abnormal accumulation of vacuolated or non-vacuolated mitochondria was also found in focal regions of some proximal axons (Fig. 7), swollen proximal axons (spheroids) and somata of degenerated anterior horn cells (Fig. 8). Rough endoplasmic reticulum and Golgi apparatus in somata were not vacuolated.

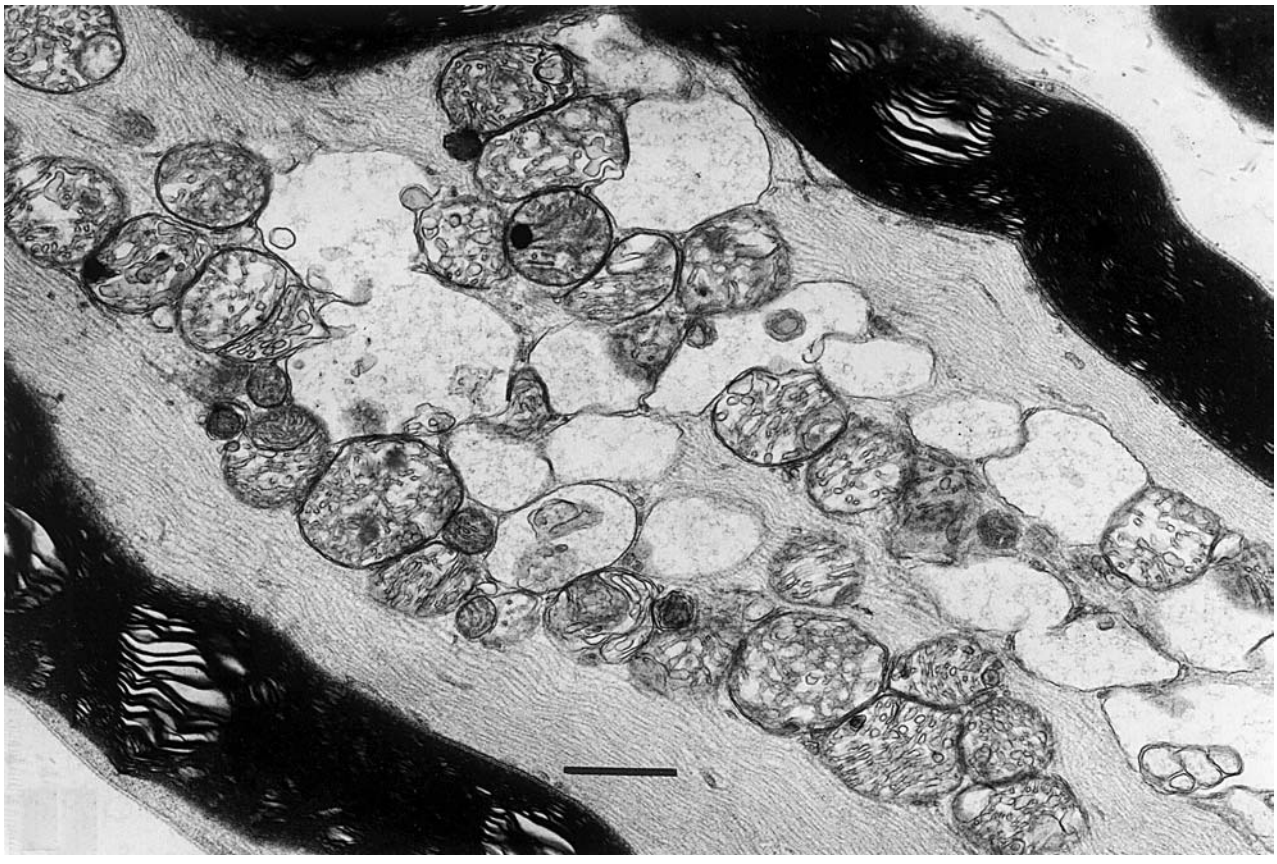

Fig. 7 Tg mouse (lumbar cord, 28 weeks). Abnormal accumulation of vacuolated and non-vacuolated mitochondria in a swollen axon of the anterior root, which contains higher levels of neurofilaments. *Bar* 1 μm

At the symptomatic stage, mitochondrial vacuolation seen in the late presymptomatic stage persisted, although to a lesser extent. Accumulation of vacuolated or non-vacuolated mitochondria was frequently observed in accumulated neurofilaments running parallel to the longitudinal section.

Most mitochondria in the somata of normal-looking anterior horn cells, proximal dendrites, axon hillock, initial segment and presynaptic terminals (Fig. 9) on the surface of the anterior horn cells showed no vacuolar changes at any stage.

Immunoelectron microscopic findings

To determine the ultrastructural distribution of human SOD1 and ubiquitin immunoreactivity, we used post-embedding immunogold electron microscopy. A rabbit polyclonal anti-human SOD1 antibody [3] at a 1:1,000 dilution and a polyclonal anti-ubiquitin antibody (DAKO) diluted at 1:500 were ideal for detection of deposits of immunogold particles in mitochondria. Mitochondria were easily identified by their characteristic structure. A high level of human SOD1-immunogold labeling was present in swollen and vacuolated mitochondria, even at presymptomatic stages (Fig. 10), but SOD1 determinants were undetectable in most normal-appearing mitochondria, except some that showed a small amount of labeling. In large vacuoles, human SOD1-immunogold labeling was predominantly observed within the electron-dense granular or amorphous material (Fig. 11). SOD1-immunogold-positive vacuolated mitochondria were almost exclusively seen in the axons; most mitochondria in proximal dendrites or somata of the anterior horn neurons were immunonegative for SOD1. Vacuolated mitochondria, or the granular or amorphous substance in vacuolated mitochondria, occasionally showed a small amount of immunogold labeling for ubiquitin (Fig. 12). Using a high dilution of anti-human SOD1 antibody (1:5,000) and anti-ubiquitin antibody (1:1,000), only granular or amorphous substance of the vacuolated space showed SOD1 and ubiquitin-immunogold deposits. In contrast, using a low dilution of these antibodies (anti-human SOD1 antibody 1:500; anti-ubiquitin antibody 1:100), not only granular or amorphous substance but also vacuolated or non-vacuolated mitochondria showed SOD1 and ubiquitin-immunogold deposits, as did other tissues occasionally and non-specifically, although to a lesser degree (Figs. 10, 11).

Discussion

Recent studies have found increasing substantial evidence for involvement of mitochondrial damage in motor neuron degeneration in familial ALS with SOD1 mutation [2,

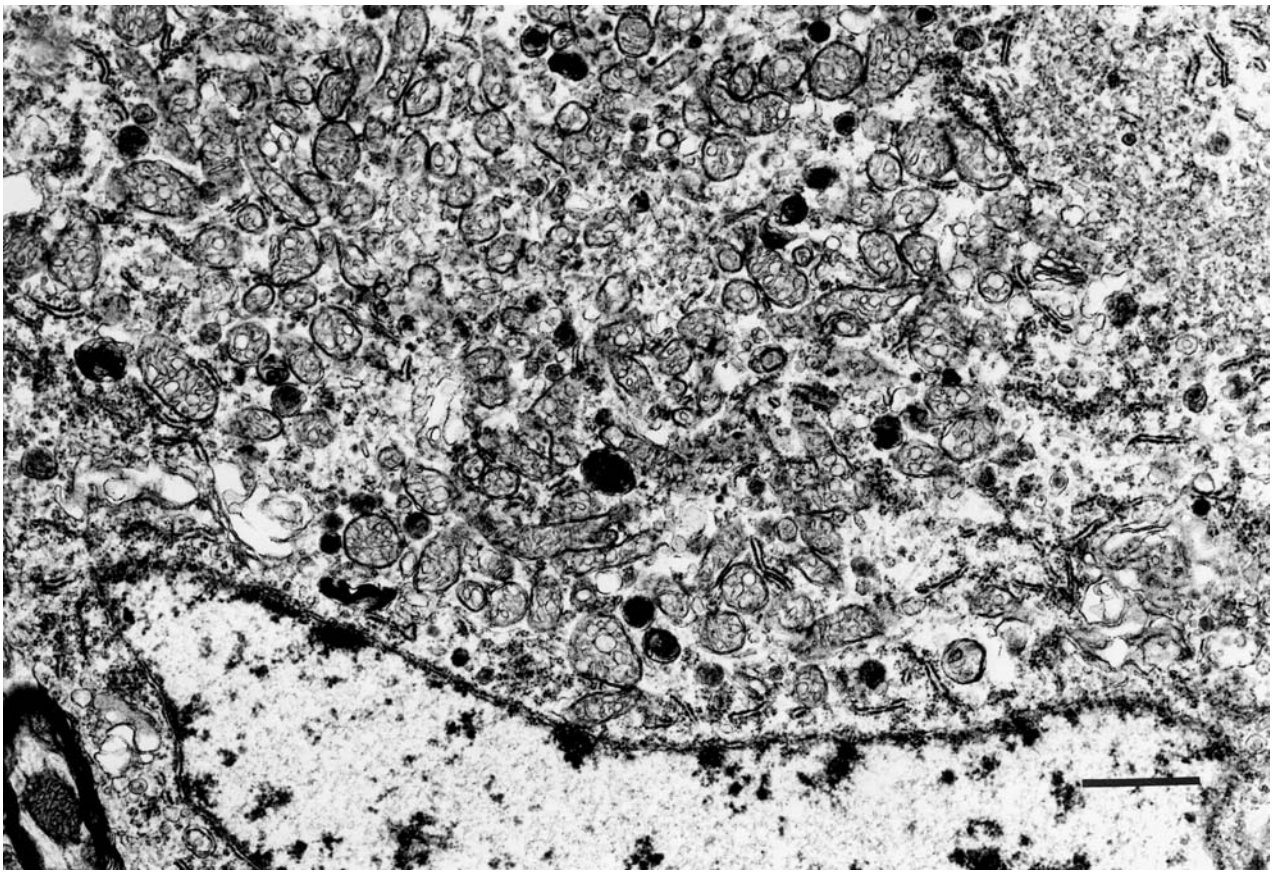

Fig. 8 Tg mouse (lumbar cord, 28 weeks). Abnormal accumulation of mitochondria is visible in the soma of a degenerated anterior horn cell. Microvacuoles are seen in the inner compartment of some mitochondria. *Bar* 1 μm

6, 14, 23, 40] and in sporadic ALS [33, 34, 39]. Morphological abnormalities of mitochondria such as bizarre giant mitochondria in liver biopsy specimens [25, 29], abnormal accumulation of mitochondria in the proximal axons [32], conglomeration of dark abnormal mitochondria at presynaptic terminals [33], and mitochondria with increased volume [34] have been reported in patients with sporadic ALS. Biochemical studies on ALS have reported functional abnormalities of mitochondria, such as changes in activity of complex I of the mitochondrial respiratory chain in familial ALS patients [6, 7], and decreased complex IV activity in patients with sporadic ALS [16]. An out-of-frame mutation of mitochondrial DNA encoding subunit I of cytochrome c oxidase has been also detected in a patient with motor neuron disease [9].

Vacuolar formation has been identified as the dominant pathological feature associated with motor neuron death and paralysis in mice expressing G93A or G37R mutant SOD1 [13, 23, 40]. However, there is a controversy regarding the origin and the site of vacuoles. Some reports propose that, in G93A SOD1 mutant mice (G1H/+ and G1L/+ lines), vacuoles originate from dilatation of rough endoplasmic reticulum in perikarya or degenerating mitochondria [12, 13], while others indicate that, in G37R and G93A SOD1 mutant mice, vacuoles are derived from degenerating mitochondria [23, 40]. With regard to the site of vacuoles, in G93A SOD1 mutant mice, vacuolated mitochondria are predominantly located in somata and their neuronal processes [13], dendrites and axons [23], or dendrites of motor neurons [20]. In G37R SOD1 mutant mice, the most clearly visible cellular abnormalities are mitochondrial vacuoles in axons and dendrites [40]. In the present study, the earliest and most prominent changes were mitochondrial swelling and vacuolar formation in the inner compartment of mitochondria, and the intermembrane space was also dilated with splitting of the outer and inner membranes, often expanding into large vacuoles, which is consistent with previous reports [12, 13, 20, 23, 39]. As a new finding, tubular or vesicular cristae increased in the somata or neuronal processes in our study. The present results, i.e., lack of vacuolar changes in mitochondria in cell body and dendrites, are intriguing and differ from other results [13, 20, 23]. It may be that an interaction between mitochondria and the cytosol is being overlooked. Probably the somatic environment is somehow more protective against the very severe changes present in the axon. Whether it is explained by fewer copies of the G93A transgene after crossing into the C57BL/6 line, or is an effect of the C57BL/6 line itself remains unknown. Actual experiments with varying transgene copy number would be required to prove this point.

Localization of SOD1-immunogold labeling of mitochondria is also open to debate. Results of some immuno-

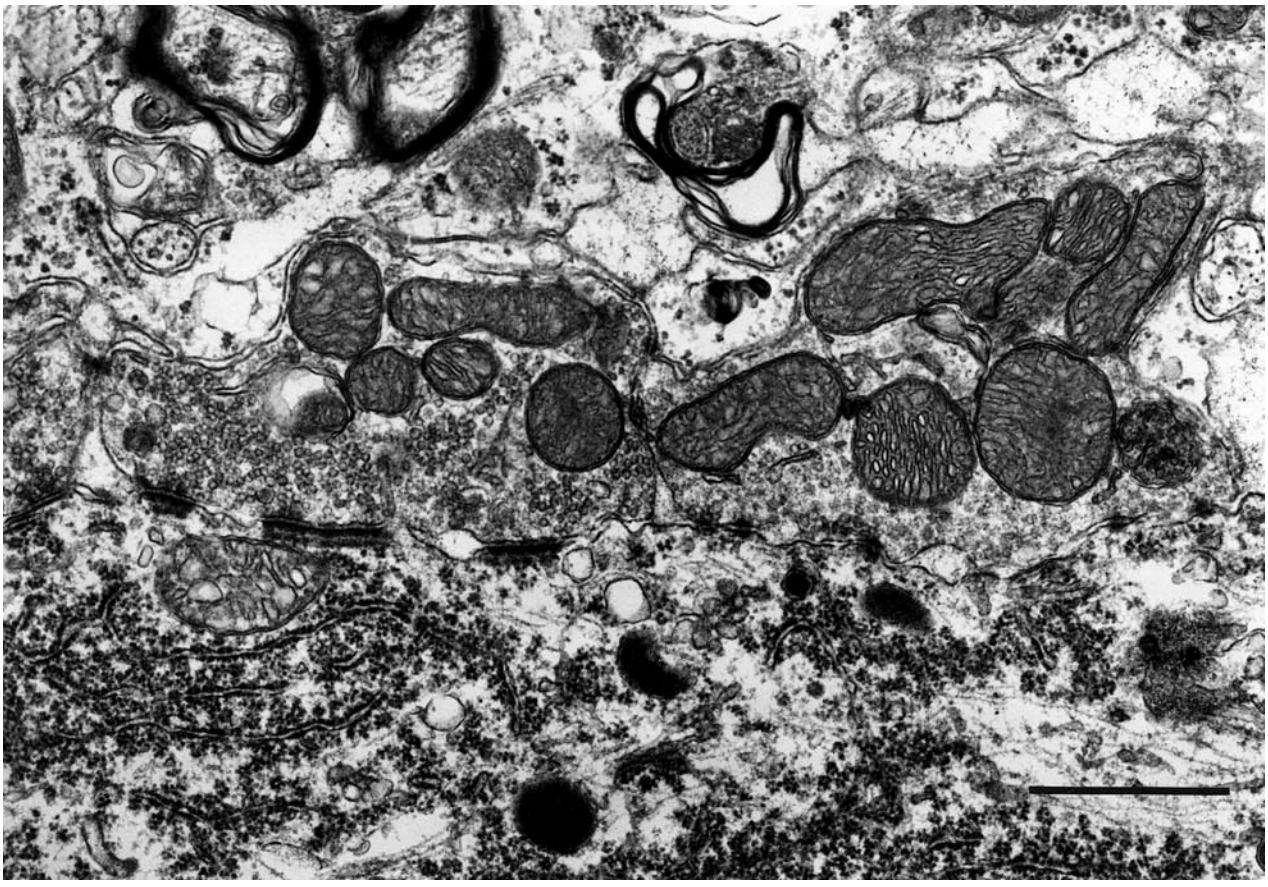

Fig. 9 Tg mouse (lumbar cord, 28 weeks). Non-vacuolated normal-appearing mitochondria in the presynaptic terminal on the surface of an anterior horn neuron. *Bar* 1 μm

electron microscopic studies indicate that SOD1 is distributed throughout the cytoplasm, in the nucleus and in peroxisomes, but not in mitochondria [10, 35]. However, other studies provide strong evidence that SOD1 is present inside mitochondria [18, 30, 36, 37], and that mutant SOD1 is associated with abnormal mitochondria in the central nervous system of mice [12, 24]. Higgins et al. [18] reported that endogenous mouse SOD1 and wild-type and mutant human SOD1 in Tg mice were located in mitochondria in the spinal cord; the intermembrane space of these mitochondria were positively stained for SOD1. They also found that far more SOD1-immunogold particles were present in mitochondria of G93A mutant mice and mice expressing wild-type human SOD1 than in mitochondria of their non-Tg littermates, and that very few, if any, SOD1-immunogold particles were present in the matrix compartment. Jaarsma et al. [20] found that a high level of SOD1-immunogold labeling was localized in swollen and vacuolated mitochondria of G93A mutant mice, and that no SOD1-immunogold labeling was present in normal-appearing mitochondria. In the present study, density of SOD1-immunogold particles increased with the progression of vacuolation in the intermembrane space and the inner compartment of vacuolated mitochondria in axons, predominantly in the granular or amorphous substance within large vacuoles, whereas no significant SOD1-immunogold particles were detected in normal-appearing mitochondria. This suggests that mitochondria are closely associated with SOD1-induced motor neuron degeneration. Differences in mutant SOD1 expression of mitochondria including non-vacuolated mitochondria may be mainly due to differences in dilution of SOD1 antibody, or in the transgene copy number.

How then does mutant SOD1 damage motor neurons? The mechanism of mitochondrial degeneration in mutant SOD1 Tg mice still remains to be elucidated, but it has been linked to correlation between oxidative damage and excitotoxicity [13, 23, 40]. Enzymatically active SOD1 is detectable in mitochondria from brain and liver of non-Tg (wild-type) animals, suggesting that SOD1 is a normal protein component of the intermembrane space [26], in which SOD1 protects mitochondria against oxidative damage, as evidenced by an increase in oxidative damage to mitochondrial proteins in yeast lacking SOD1 [30, 36]. The toxicity of mutant SOD1 may involve increased production of reactive oxygen and nitrite species, such as hy-

Fig. 10 **A** Tg mouse (cervical cord, 30 weeks). Human SOD1-immunogold labeling is present in vacuolated mitochondria at the presymptomatic stage. A small amount of labeling was also observed in adjacent areas such as non-vacuolated mitochondria and filamentous structure. **B** Control for comparison: almost none of the non-vacuolated mitochondria exhibit SOD1-immunogold deposits. *Bar* 1 μm ▶

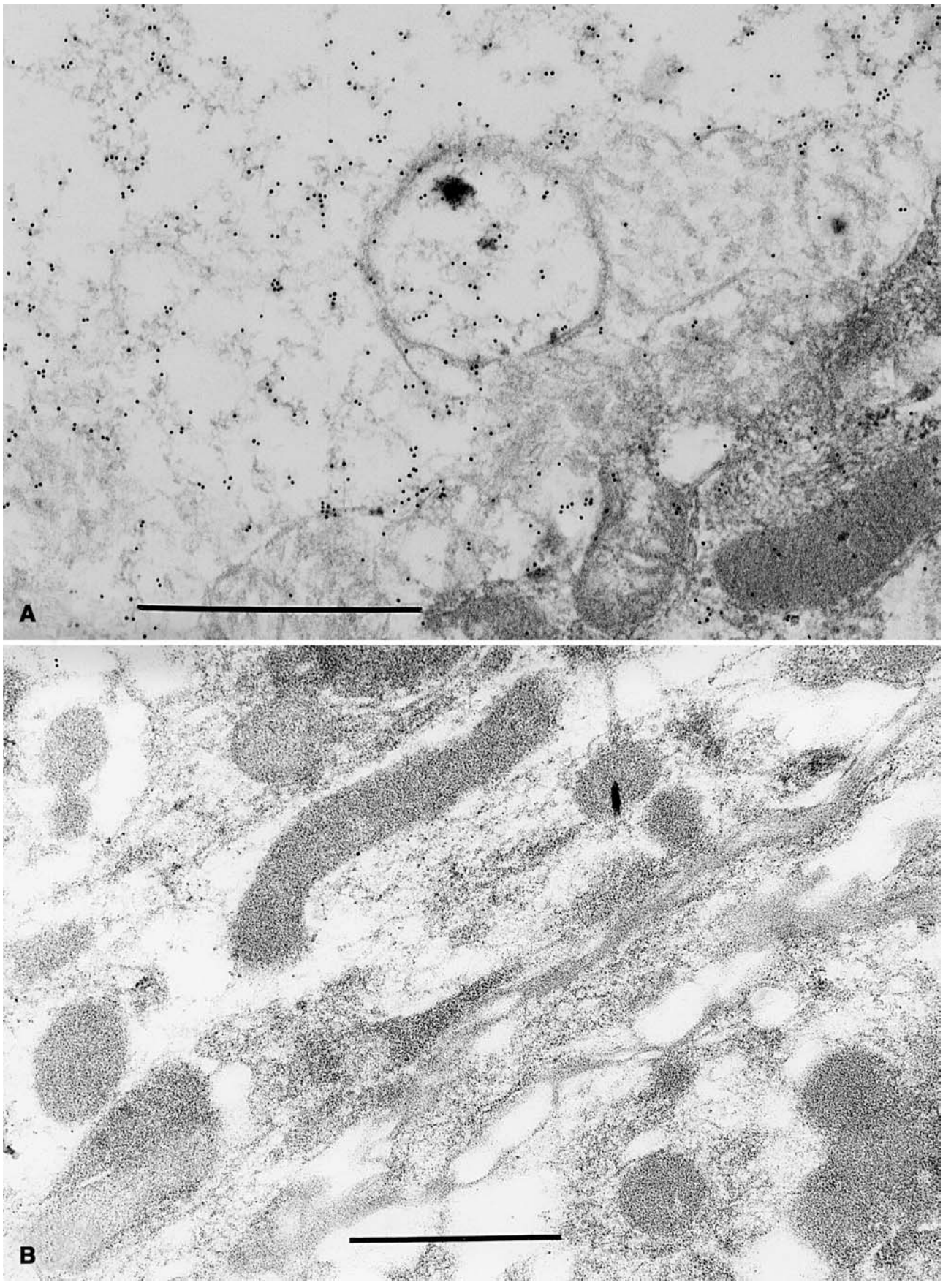
A
B

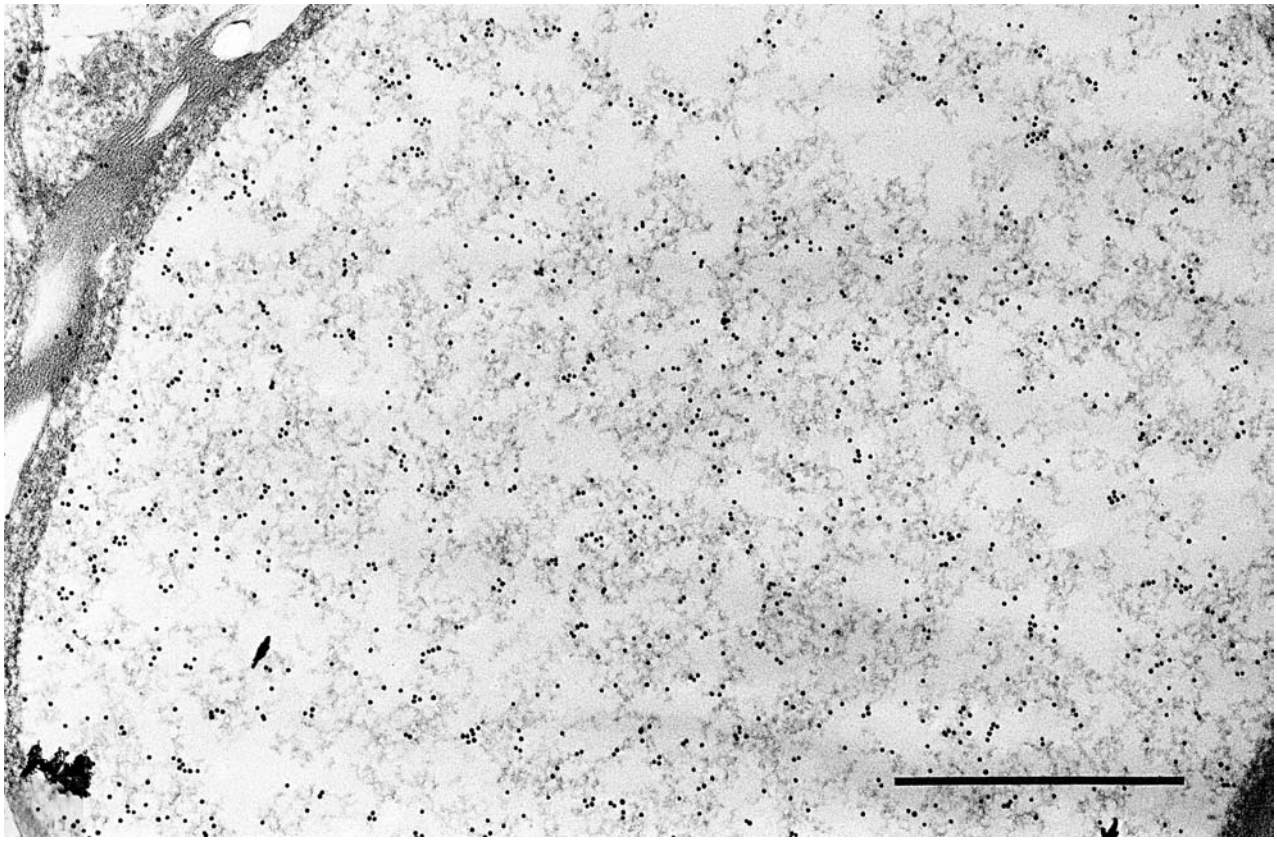

Fig. 11 Tg mouse (cervical cord, 30 weeks). In large vacuoles, prominent human SOD1-immunogold labeling is present in the electron-dense granular or amorphous substance. A low level of SOD1-immunogold deposits was also observed in adjacent areas. *Bar* 1 μm

droxyl radicals and peroxynitrite [15, 38]. Mitochondrial dysfunction also increases production of reactive oxygen species, which damage major cellular components, such as nucleic acids, lipids and proteins [1]. Mitochondrial damage results in energy deficiency, leading to reduced activity of ATP-dependent ionic pumps, which in turn is responsible for ionic imbalance in cells [4]. Thus, one mechanism by which mutant SOD1 causes motor neuron injury may involve inhibition of specific components of the mitochondrial respiratory chain [28]. Mitochondrial dysfunction can lead to increased cytosolic calcium levels as a result of cellular depolarization [27], probably resulting in motor neuron death, because large motor neurons do not contain calcium-binding proteins such as parvalbumin and calbindin D-28k and are less able to buffer calcium [19]. Of particular interest is the finding that vulnerability of motor neurons to excitotoxicity is selectively enhanced when mitochondrial function is impaired [22].

Our results show the disruption of the inner membrane to which the enzymes of the respiratory chain attach, and the expansion of the intermembrane space, predominantly in the proximal axons, even at the early presymptomatic stage. The expansion of the intermembrane space in our study is consistent with the previous report that mutant SOD1 damages mitochondrial membranes, causing extension and leakage of the outer membrane and expansion of the intermembrane space [41]. This study also reveals that SOD1 activity increases in mitochondrial vacuoles with disease progression, but it is not detected in normal-appearing mitochondria. Although we can not rule out the possibility that SOD1 expression within mitochondria is simply leaking in from the cytosol in damaged organelles, it is likely that mitochondria acquire increased SOD1 activity due to the overexpression of mutant SOD1, resulting in cellular toxicity and vacuolar formation. In other words, the toxicity of mutant SOD1 directly affects mitochondria, which causes a decrease in ATP that in turn disrupts the axonal transport of substrates needed for neuronal viability, thus leading to motor neuron degeneration. Abundant SOD1-immunogold labeling in mitochondrial vacuoles may be associated with disturbed SOD1 protein turnover in vacuoles, causing the gradient of mutant SOD1 protein concentration between the inside and the outside of mitochondria. The localization of ubiquitin with SOD1 in some vacuolated mitochondria also suggests that protein degradation by ubiquitin-proteasomal system may be also disrupted by several pathomechanisms, such as decreased processing of ubiquitinated proteins due to impairment of mitochondrial function or of proteasomal function, both of which are caused by mutant SOD1. Moreover, giant vacuoles occupying almost the entire axonal caliber could be another contributing factor in motor neuron degeneration, in that they physically block axonal

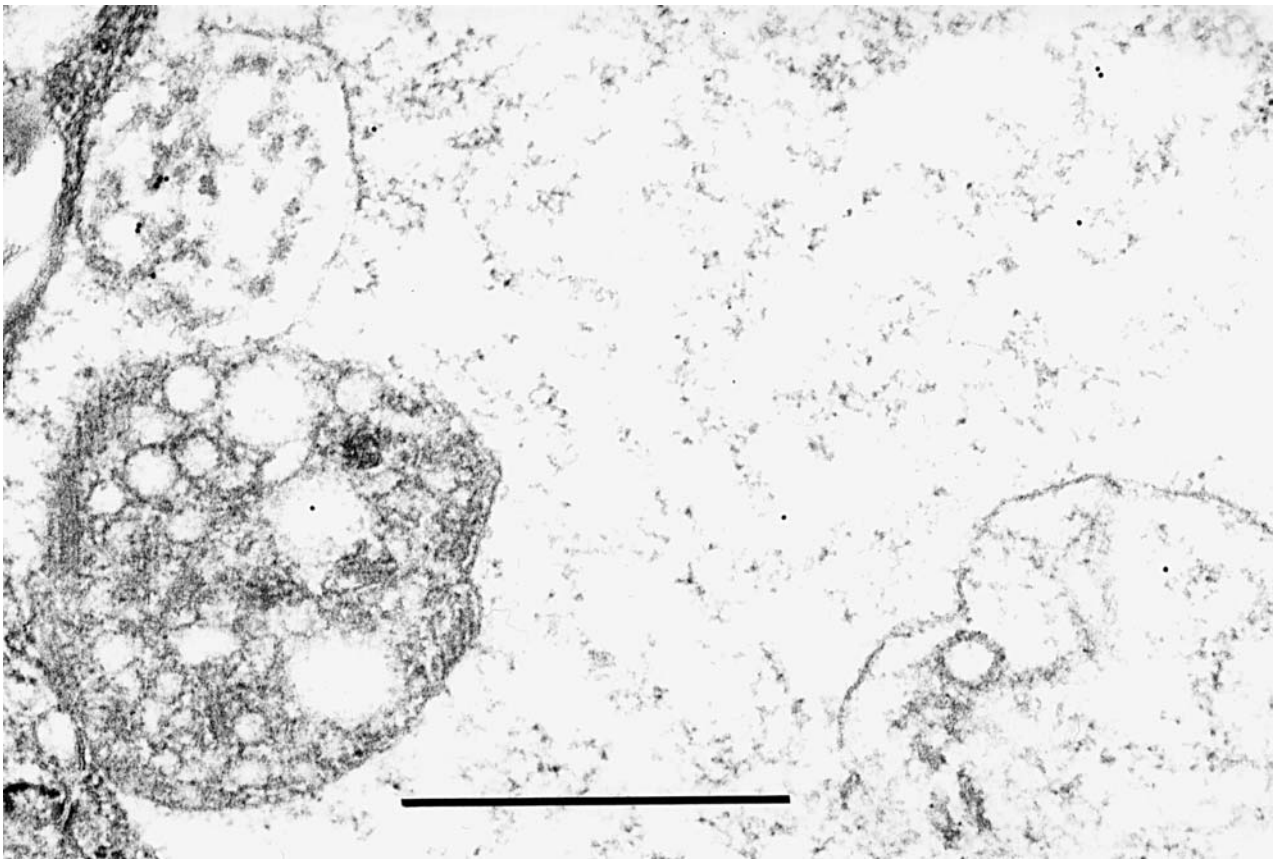

Fig. 12 Tg mouse (lumbar cord, 30 weeks). Degenerated or vacuolated mitochondria and granular substance of a large vacuolation show a small amount of immunogold labeling for ubiquitin. *Bar* 1 μm

transport. Thus, whether it is a primary or secondary event, mitochondrial dysfunction appears to play a pivotal role in the processes of selective motor neuron death in the present animal model.

Acknowledgements This work was supported by a Grant-in-Aid for General Scientific Research (C) from the Japanese Ministry of Education, Science and Culture, and by a grant from the Japan ALS Association. We gratefully acknowledge the technical assistance of Dr. N. Shibata and Mr. M. Karita (Department of Pathology, Tokyo Women's Medical University, Tokyo) in immunoelectron microscopy.

References

1. Andreassen OA, Ferrante RJ, Klivenyi P, Klein AM, Shinobu LA, Epstein CJ, Beal MF (2000) Partial deficiency of manganese superoxide dismutase exacerbates a transgenic mouse model of amyotrophic lateral sclerosis. Ann Neurol 47:447–455
2. Andreassen OA, Ferrante RJ, Klivenyi P, Klein AM, Dedeoglu A, Albers DS, Kowell NW, Beal MF (2001) Transgenic ALS mice show increased vulnerability to the mitochondrial toxins MPTP and 3-nitropropionic acid. Exp Neurol 168:356–363
3. Asayama K, Janco RL, Burr IM (1985) Selective induction of manganous superoxide dismutase in human monocytes. Am J Physiol 249:C393–C397
4. Beal MF (1992) Does impairment of energy metabolism result in excitotoxic neuronal death in neurodegenerative illnesses? Ann Neurol 1:119–130
5. Borthwick GM, Johnson MA, Ince PG, Shaw PJ, Turnbull DM (1999) Mitochondrial enzyme in amyotrophic lateral sclerosis: implications for the role of mitochondria in neuronal cell death. Ann Neurol 46:787–790
6. Bowling AC, Schulz JB, Brown RH, Beal MF (1993) SOD activity, oxidative damage, and mitochondrial energy metabolism in familial and sporadic ALS. J Neurochem 61:2322–2325
7. Browne SE, Bowling AC, Baik MJ, Gurney M, Brown RH Jr, Beal MF (1998) Metabolic dysfunction in familial, but not sporadic, amyotrophic lateral sclerosis. J Neurochem 71:281–287
8. Carri MT, Ferri A, Battistoni A, Famhy L, Cabbianelli R, Poccia F, Rotilio G (1997) Expression of a Cu, Zn superoxide dismutase typical of familial amyotrophic lateral sclerosis induces mitochondrial alteration and increase of cyotosolic Ca^{2+} concentration in transfected neuroblastoma SH-Sy5Y cells. FEBS Lett 414:365–368
9. Comi GP, Bordoni A, Salani S, Franceschina L, Sciacco M, Prelle A, Fortunato F, Zeviani M, Napoli L, Bresolin N, Moggio M, Ausenda CD, Taanman J-W, Scarlato G (1998) Cytochrome c oxidase subunit I microdeletion in a patient with motor neuron disease. Ann Neurol 43:110–116
10. Crapo JD, Oury T, Rabouille C, Slot JW, Chang LY (1992) Copper, zinc superoxide dismutase in primarily a cytosolic protein in human cells. Proc Natl Acad Sci USA 89:10405–10409
11. Curti D, Malaspina A, Facchetti G, Camana C, Mazzini L, Tosca P, Zerbi F, Ceroni M (1996) Amyotrophic lateral sclerosis: oxidative energy metabolism and calcium homeostasis in peripheral blood lymphocytes. Neurology 47:1060–1064
12. Dal Canto MC, Gurney ME (1994) Development of central nervous system pathology in a murine transgenic model of human amyotrophic lateral sclerosis. Am J Pathol 145:1271–1280

13. Dal Canto MC, Gurney ME (1995) Neuropathological changes in two lines of mice carrying a transgene for mutant human Cu, Zn SOD, and in mice overexpressing wild-type human SOD: a model of familial amyotrophic lateral sclerosis (FALS). Brain Res 676:25–40
14. Dhaliwal GK, Grewal RP (2000) Mitochondrial DNA deletion mutation levels are elevated in ALS brains. Neuroreport 11: 2507–2509
15. Estevez AG, Crow JP, Sampson JB, Reiter C, Zhuang YX, Richardson GJ, Tarpey MM, Barbeito L, Beckman JS (1999) Induction of nitric oxide-dependent apoptosis in motor neurons by zinc-deficient superoxide dismutase. Science 286:2498–2500
16. Fujita K, Yamauchi M, ShibayamaK, Ando M, Honda M, Nagata Y (1996) Decreased cytochrome c oxidase activity but unchanged superoxide dismutase and glutathione peroxidase activities in the spinal cords of patients with amyotrophic lateral sclerosis. J Neurosci Res 45:276–281
17. Gurney ME, Pu H, Chiu AY, Dal Canto MC, Polchow CY, Alexander DD, Caliendo J, Hentati A, Kwon YW, Deng HX, et al (1994) Motor neuron degeneration in mice that express a human Cu/Zn superoxide dismutase mutation. Science 264:1772–1775
18. Higgins CMJ, Jung C, Ding H, Xu Z (2002) Mutant Cu, Zn superoxide dismutase that causes motoneuron degeneration is present in mitochondria in the CNS. J Neurosci 22:RC215
19. Ince P, Stout N, Shaw P, Slade J, Hunziker W, Heizmann CW, Baimbridge KG (1993) Parvalbumin and calbindin D-28k in the human motor system and in motor neuron disease. Neuropathol Applied Neurobiol 19:291–299
20. Jaarsma D, Rognoni F, Duijn W van, Verspaget HW, Haasdijk ED, Holstege JC (2001) CuZn superoxide dismutase (SOD1) accumulates in vacuolated mitochondria in transgenic mice expressing amyotrophic lateral sclerosis-linked SOD1 mutations. Acta Neuropathol 102:293–305
21. Jung C, Higgins CMJ, Xu Z (2002) Mitochondrial electron transport chain complex dysfunction in a transgenic mouse model for amyotrophic lateral sclerosis. J Neurochem 3:535–545
22. Kaal EC, Vlug AS, Versleijen MW, Kuilman M, Joosten EA, Bar PR (2000) Chronic mitochondrial inhibition induces selective motoneuron death in vitro: a new model for amyotrophic lateral sclerosis. J Neurochem 74:1158–1165
23. Kong J, Xu Z (1998) Massive mitochondrial degeneration in motor neurons triggers the onset of amyotrophic lateral sclerosis in mice expressing a mutant SOD1. J Neurosci 18:3241–3250
24. Levine JB, Kong J, Nadler M, Xu Z (1999) Astrocytes interact intimately with degenerating motor neurons in mouse amyotrophic lateral sclerosis (ALS). Glia 28:215–224
25. Masui Y, Mozai T, Kakehi K (1985) Functional and morphometric study of the liver in motor neuron disease. J Neurol 232:15–19
26. Mattiazzi M, D'Aurelio M, Gajewski CD, Martushova K, Kiaei M, Beal MF, Manfredi G (2002) Mutated human SOD1 causes dysfunction of oxidative phosphorylation in mitochondria of transgenic mice. J Biol Chem 277:29626–29633
27. McLaughlin BA, Nelson D, Silver IA, Erecinska M, Chesselet MF (1998) Methylmalonate toxicity in primary neuronal cultures. Neuroscience 86:279–290
28. Menzies FM, Cookson MR, Taylor RW, Turnbull DM, Chrzanowska-Lightowlers ZMA, Dong L, Figlewicz DA, Shaw PJ (2002) Mitochondrial dysfunction in a cell culture model of familial amyotrophic lateral sclerosis. Brain 125:1522–1533
29. Nakano K, Hirayama K, Terao K (1987) Hepatic ultrastructural changes and liver dysfunction in amyotrophic lateral sclerosis. Arch Neurol 44:103–106
30. Okado-Matsumoto A, Fridovich I (2001) Subcellular distribution of superoxide dismutase (SOD) in rat liver: Cu, Zn-SOD in mitochondria. J Biol Chem 276:38388–38393
31. Rosen DR, Siddique T, Patterson D, Figlewicz DA, Sapp P, Hentati A, Donaldson D, Goto J, O'Regan JP, Deng HX, et al (1993) Mutations in Cu/Zn superoxide dismutase gene are associated with familial amyotrophic lateral sclerosis. Nature 362:59–62
32. Sasaki S, Iwata M (1996) Impairment of fast axonal transport in the proximal axons of anterior horn neurons in amyotrophic lateral sclerosis. Neurology 47:535–540
33. Sasaki S, Iwata M (1996) Ultrastructural study of synapses in the anterior horn neurons of patients with amyotrophic lateral sclerosis. Neurosci Lett 204:53–56
34. Siklos L, Engelhardt J, Harati Y, Smith RG, Joo F, Appel SH (1996) Ultrastructural evidence for altered calcium in motor nerve terminals in amyotrophic lateral sclerosis. Ann Neurol 39:203–216
35. Slot JW, Geuze HJ, Freeman BA, Crapo JD (1986) Intracellular localization of the copper-zinc and manganese superoxide dismutases in rat liver parenchymal cells. Lab Invest 55:363–571
36. Sturtz LA, Diekert K, Jensen LT, Lill R, Culotta VC (2001) A fraction of yeast Cu, Zn-superoxide dismutase and its metallochaperone, CCS, localize to the intermembrane space of mitochondria. a physiological role for SOD1 in guarding against mitochondrial oxidative damage. J Biol Chem 276:38084–38089
37. Weisiger RA, Fridovich I (1973) Mitochondrial superoxide dismutase. Site of synthesis and intramitochondrial localization. J Biol Chem 248:4793–4796
38. Wiedau-Pazos M, Goto JJ, Rabizadch S, Gralla EB, Roc JA, Lee MK, Valentine JS, Bredesen DE (1996) Altered reactivity of superoxide dismutase in familial amyotrophic lateral sclerosis. Science 271:515–518
39. Wiedemann FR, Manfredi G, Mawrin C, Beal MF, Schon EA (2002) Mitochondrial DNA and respiratory chain function in spinal cords of ALS patients. J Neurochem 80:616–625
40. Wong PC, Pardo CA, Borchelt DR, Lee MK, Copeland NG, Jenkins NA, Sisodia SS, Cleveland DW, Price DL (1995) An adverse property of a familial ALS-linked SOD1 mutation causes motor neuron disease characterized by vacuolar degeneration of mitochondria. Neuron 14:1105–1116
41. Xu ZS, Higgins CMJ (2002) Mechanism of mitochondrial vacuolation in a transgenic mouse model for ALS. Amyotroph Lateral Scler other Motor Neuron Disord 3 (Suppl 2):26–27